

# Remote Sensing Image Compression using Two Dimensional Dual Tree Complex Wavelet Transform with Fuzzy Inference Filter

Sudhakar Ilango S.\* and Seenivasagam V.\*\*

## ABSTRACT

**Background:** The real-time remote sensing image provides an evolution in compression approaches in both the practical and theoretical value. With the basic characteristics like statistical analysis and decomposed image, a significant compression technique has been developed for remote sensing image of the sub-image.

**Material and Methods:** To aid remote sensing image compression, a compression algorithm named 2D-Dual Tree-Complex Wavelet Transform (2D-DT-CWT) is proposed. Three directions are considered for analysis of image, i.e. vertical, horizontal and diagonal. Here, for the intention of image compression, transform direction based on geometric curve is measured. A method named Fuzzy Inference Filter (FIF) is utilized for to compute the entropies of sub band coefficients. To encode the wavelet coefficient a Context-adaptive binary arithmetic coding (CABAC) through Lattice Vector Quantization (LVQ) is offered.

**Result:** The experimentation shows that the 2D-DT-CWT provides a improvement in remote sensing images particularly in transform coding gain with high resolution.

**Conclusion:** The comparative study on the existing 2-D Oriented Wavelet Transform (2D-OWT) and JPEG2000 is made. Added, the memory required for operational process is lesser and the new compression technique is simpler.

## 1. INTRODUCTION

The evolution of remote sensing image from initial magnitude of MB to the current magnitude GB and even to TB saw an increasing growth in the modern remote sensing technology. Added, the data are stored in the structure of photographs, with the limited internet's bandwidth, the use of gathering the remote sensing image pretense pressure on its evaluation, own storage and transmission and has become an restricted use of remote sensing data extensively. To solve the above mentioned problem, the dependency of computer hardware with increased speed, increased network bandwidth, expanding the capacity of the storage devices along with the image compression technique. Thus by increasing the storage capacity with bandwidth, proceeding with image compression, image transmission or storage and quantitative data has made small. The image compression technique helps in reducing the cost and hardware requirements such as effective image compression and stable remote sensing image application act as a vital role in successful application Khashman et al. (2008).

The benefits provided by remote sensing image compression are listed below: (1) obtaining channel with less cost and quick transmission of multiplicity of sources (2) opening multiple equivalent operations with the previously available communication lines (3) reducing the transmitter power (4) reducing the cost

\* Assistant Professor, Department of CSE, Sri Krishna College of Engineering and Technology, Coimbatore, Email: sudhakar.ilango@gmail.com

\*\* Professor, Department of CSE, National Engineering College, Thoothukudi-628 503

of storage and chop the data storage capacity. Thus for the remote sensing application, image compression helps in saving the storage capacity and channel capacity throughout the entire transmission time, to improve the storage, handling and transmission efficiency was studied Debnath et al. (2008).

The image being uncompressed in a remote sensing can be very huge. The sensor has the ability to collect numerous gigabytes of data a day. Compression is thereby becomes more important to facilitate both transmission and storage of remote sensing images. Gathering of remote sensing images are performed on acquisition platforms, such as satellites and earth observations. Thus compression techniques provide an impact on the remote sensing applications. Owing with the utilization of image characters and statistical correlations by affording the compacted representation of the signals provides a effective image compression. For the past few years, many transforms have been build up for providing a successful image compression Penna et al.(2007), such as Discrete Cosine Transform (DCT), Karhunen-Loeve transform (KLT) and Discrete Wavelet Transform (DWT).

JPEG200 Taubman et al. (2001) has been proposed to offer an element with high-quality frequency resolution at stumpy frequency when proffer elements with high-quality resolution in higher frequency concurrently. To perform high presentation scalable image compression Taubman (2000) an Embedded Block Coding with Optimal Truncation (EBCOT) algorithm is proposed. 2D-Oriented Wavelet Transform (OWT) and JPEG2000 are compression techniques based on DWT. For the past few decades, embedded bit-plane coding techniques and application based DWT are most popular. Compression is a popular technique to reduce the amount of data to transmitted or saved by the receiver channel.

In this work, for performing remote sensing image compression, an algorithm named 2D-Dual Tree-Complex Wavelet Transform (DT-CWT) is presented. Here, examination of images is performed on three different directions like vertical, horizontal and diagonal. The image compression measurement named geometric curve based transform is performed here. To determine whether the coefficient is noteworthy or not, this method uses Fuzzy Inference Filter (FIF) for calculating the entropies of the sub band coefficients. To encode the wavelet significant coefficient a Context-adaptive binary arithmetic coding (CABAC) with Lattice Vector Quantization (LVQ) is presented. The experimentation shows that the proposed 2D-DT-CWT provides a noteworthy improvement in remote sensing images particularly in transform coding gain with high resolution. The comparative study on the existing 2-D Oriented Wavelet Transform (2D-OWT) and JPEG2000 is made with the proposed system.

The association of the remaining content of the paper is as follows: In section 2 background study of CWT is taken for conversation. In section 3 spotlight the 2D-Dual Tree-Complex Wavelet Transform (DT-CWT) based image compression algorithm. In section 4 the experimental results and discussion are accessible with image compression methods. Finally, in section 5, the conclusion and future work is discussed.

## 2. COMPLEX WAVELET

The sampled Discrete Wavelet Transform (DWT) has been related to the extensive range of signal processing operations successfully. But the performance is limited based on the following issues (Selesnick et al. 2005).

- Coefficient oscillations at singularity (zero crossings)
- Shift variance cause small change in the given input leads to higher change in the output.
- Aliasing is cancelled due to non-ideal filtering and down sampling by the synthesis filter except when the coefficient remains unchanged.
- Due to the absence of directional selectivity in higher dimensions, e.g. competent to distinguish edge orientation between + 450 and – 450.

To overcome the shift dependence problem, consider the utilization of undecimated DWT (over-complete), without determining the directional selectivity problem. Another approach that inspires the

Fourier transforms whose phase offset and shift invariant do the shift encoding. The large coefficient magnitude point out the singularity existence similarly the phase indicates the position with respect to the wavelet support in a wavelet transform. The complex wavelets transform (CWT) utilizes quadrature or analytic wavelets which provide guaranteed shift invariance, magnitude phase representation and no aliasing Grgic et al. (2001). At present, the complex-valued wavelet transforms CWT have been used for improving the DWT deficiencies, with the availing Dual-Tree CWT (DT-CWT) Selesnick et al. (2005) which becomes a desired approach based on its easy implementations. In the DT-CWT, the wavelet filters give way for the real and the imaginary part transform with the parallel decomposition tree, by allowing the real-valued wavelet implementations and its methodologies to prove. The DT-CWT provides a significant merit having higher degree of directionality compared to the conventional DWT with response to the decomposition. Eventually, both the trees are biorthogonal or orthonormal decompositions, the DT-CWT is considered as redundant tight frame completely.

To form a Hilbert transform (HT) pair, an analytic wavelet  $\psi_c(t)$  consists of two real wavelets  $\psi_r(t)$  and  $\psi_i(t)$  representing that they are orthogonal, i.e. shifting to  $\pi/2$  in the complex plane Barbara Penna et al. (2007).

$$\psi_c(t) = \psi_r(t) + j \psi_i(t)$$

$$\psi_i(t) = HT\{\psi_r(t)\} = \frac{1}{\pi} \int_{-\infty}^{\infty} \frac{\psi_r(\tau)}{t-\tau} d\tau = \psi_r(t) * \frac{1}{\pi t}$$

And for their Fourier transform pairs  $H_r(\omega)$  and  $H_i(\omega)$

$$H_i(\omega) = FT\{HT\{\psi_r(t)\}\} = -j \cdot \text{sgn}(\omega) H_r(\omega)$$

To produce the complicated results in the CWT, the analytic or quadrature formulation concept is employed with the filter bank structure of standard DWT. By satisfying the necessary convergence condition, a design technique is formulated to substitute the real-valued filter coefficients with the Complex-valued coefficients. Later, complex filter is then crumbled into two real-valued filters. To form a Hilbert transform pair, two real-valued filters provide corresponding impulse responses in quadrature. An analytic filter is formed with the combined pair of filters. The interpretation and formulation of analytic filter is shown in fig (1).

### 3. MATERIAL AND METHODS

The new compression technique named 2D-Dual Tree-Complex Wavelet Transform (DT-CWT) based image compression algorithm is presented in this section. Employing Fuzzy Inference Filter (FIF) for coefficient selection in DT-CWT is also presented here.

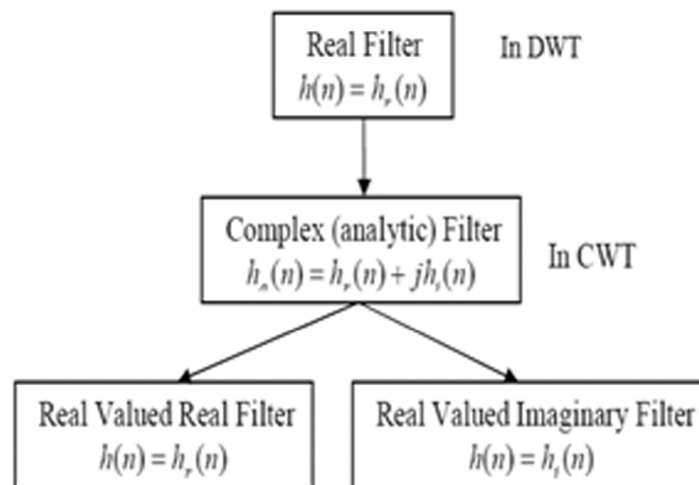


Figure 1: Analytic Filter

The complete structure of the proposed method is illustrated in fig 2. Initially in the first step, remote source image is selected and the direction finder is employed to find the transform direction. Using DT-CWT, image decomposition into wavelet coefficients ( $w$ ) is conducted. The coefficient  $w$ , modifies employing threshold. To determine whether the coefficient is important or not, FIF is applied to the for sub band coefficients. To encode the wavelet significant coefficients, Context-adaptive binary arithmetic coding (CABAC) with Lattice Vector Quantization (LVQ) is utilized here. With the use of inverse DT-CWT and FIF decoding, the reconstructing of image is performed.

**3.1. Directional Detection**

In general, the position of the image block is given by three categories: 1) a smooth block with intensities in a relative scale is uniform 2) an geometry block where the block consists of edge and 3) a texture block, where the block comprises of pseudorandom or texture or random pattern. In case 1, a smooth area in an image is observed without showing any prominent direction. In case 2, there exist some predominant directions, used for image compression. Finally, the texture pixels and edge should be recognized for determining the directions.

Geometric features such as edges implies on transition between the textured or smooth regions and are characterized by abstract variation in intensity which continues along curved or straight contours. Edge helps in communicate to the significant information, thus providing the shape and position of the pictured objects and many other features. The pixel value changes quickly with the orthogonal direction of the edges. Image high frequency energy gets started from the edges. For the above stated reason, an algorithm for compression of image is stated successfully with encoded geometric features.

A wavelet coefficients in geometric regions is represented with respect to DTCWT, 20 is the representation of collected geometric atoms which builds linear approximation piecewise to contours. The inherent model of the DTCWT representation is given coherently amongst the geometric wavelet coefficients. By modeling the simplest geometry type, a proposed method starts with: straight, sharp edge and isolated.

In a wavelet dual tree, consider a node  $i$ . by constructing the tree a and tree b in a dyadic block  $B_i$ , the wavelet coefficient of a real and an imaginary tree is rooted at I, by projecting the wavelet domain. Also, the dual tree is not the one and only available geometric description on  $B_i$ . By permitting tiling of real and

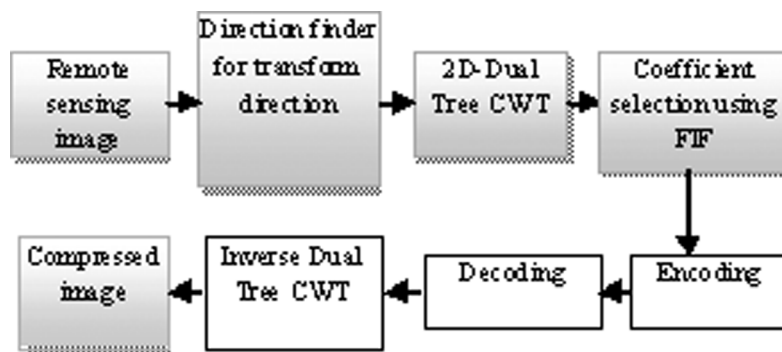


Figure 2: Overall of Procedure of Proposed Method

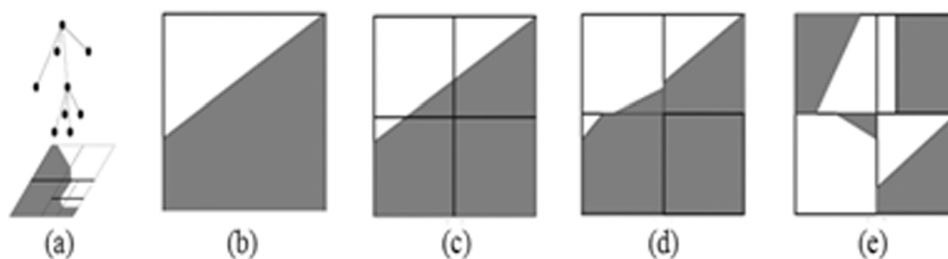


Figure 3: A dual tree disintegration

imaginary tree, dual tree decomposition is brought to use, describing the geometry on Bi. To achieve a precise approximation of wavelet coefficients downwards from in a particular wavelet domain. For encoding dual tree decomposition, effective approaches are designed here.

Fig 3 shows (a) A dual tree disintegration can be understand as a pruned tree a, tree b, where each node comprises a leaf nodes and set of dual tree parameters specify the depiction. (b) Trees provided on a dyadic block. (c) Predictions of block's children, measured to be their most probable arrangement. (d) A slightly less likely arrangement for the children. (e) A significantly less likely arrangement.

### 3.2. Image Compression Using 2D-DTCWT

Data compression is essential in transmission of information and storage. Predominantly digital image compression is of large significance because of the high storage and transmission necessities. By the elimination of the redundant data, the demonstration of the image can be given in a smaller number of bits and thus can be condensed. Several compression techniques have been initiated in recent decades for accomplishing better compression. This study will spotlight on transform coding and then particularly on Wavelet Transform coefficients which will make only small assistance to the information contents that can be unobserved. Generally the image is separated into blocks (sub images) of 8x8 or 16x16 pixels, and then every block in discrete cosine transform is distorted in separate. But this does not think about any correlation between blocks, and generates "blocking artifacts", which are not enviable in case a smooth image is required.

2D- dual tree complex wavelets transform is utilized over complete images, in place of sub images, so that it doesn't construct any blocking artifacts. This is a enormous benefit of wavelet compression in contrast other transform compression method. In wavelet coefficient, the real and imaginary noteworthy and not important are noticed by FIF. For few signals, a number of wavelet coefficients are close up to or virtually equal to zero and even the Threshold be able to do the alteration of the coefficients for constructing additional zeros. In Hard thresholding any coefficient underneath a threshold  $\lambda$ , is set to zero which, in turn, creates many concurrent zeros which can be put aside in lesser space, and broadcasted quicker by the utilization of entropy coding compression. This demonstrates that the wavelet analysis doesn't really squeeze a signal. It merely gives information about the signal thus permitting the data to be packed in by standard entropy coding method. In hard threshold, the input is kept if it is better than the threshold; else it is set to zero. The wavelet thresholding process eradicates noise by thresholding the wavelet coefficients of the comprehensive sub bands only, at the same time observance of low resolution coefficients unchanged Jacob et al. (2004). So, selecting the threshold level is an significant operation such that the coefficients owns magnitude superior than threshold are extravagance as signal of attention and remain the same or alter it in accord with the kind of threshold selected and the remaining coefficients become zero. The image is then renovated from the tainted coefficients. This process is also known as the inverse dual tree complex wavelet transforms (IDWT).

### 3.3. 2D DT-CWT

The 2D DT-CWT also distinguishes the characteristics of different orientations more precisely. While on the divergent, the critically decimated 2D DWT provides the output of three direction selective sub-bands per level thus assigning image features which are tilting at the angles of  $90^\circ$ ,  $\pm 45^\circ$ , and  $090^\circ$ , the 2D DT-CWT results in six directional sub bands per level for enlightening the information of an image in  $\pm 15^\circ$ ,  $\pm 45^\circ$  and  $\pm 75^\circ$  directions with 4:1 repeatedly.

The accomplishment of 2-D DTCWT consists of two steps. First, an input image is festering up to a requisite level by two separable 2D DWT branches, branch and branch  $b$ , whose filters are mainly intended to convince the Hilbert pair prerequisite. Then six high-pass sub bands are fashioned at each level  $Hla$ ,  $Lha$ ,  $Hha$ ,  $HLb$ ,  $LHb$  and  $HHb$ . Next, every two equivalent sub bands poses same pass-bands are linearly joined either by averaging or differencing. Consequently, sub bands of 2D DT-CWT at each level are established as

$$\frac{LH_a + LH_b}{\sqrt{2}}, \frac{LH_a - LH_b}{\sqrt{2}}, \frac{HL_a + HL_b}{\sqrt{2}},$$

$$\frac{HL_a - HL_b}{\sqrt{2}}, \frac{HH_a + HH_b}{\sqrt{2}}, \frac{HH_a - HH_b}{\sqrt{2}},$$

The six wavelets are distinct by tilting shown above having the sum/difference operation is orthonormal, comprises a perfect reconstruction wavelet transform. The imaginary part of 2D DT-CWT has the similar basis function as that of real part. The 2D DT-CWT structure has an addition of conjugate filtering in 2D case. The filter bank structure of 2D dual-tree is demonstrated in figure (4).

2D structure requires four trees for examination as well as for synthesis. The pairs of conjugate Filters are functional to two dimensions (x and y) directions, which can be uttered as:

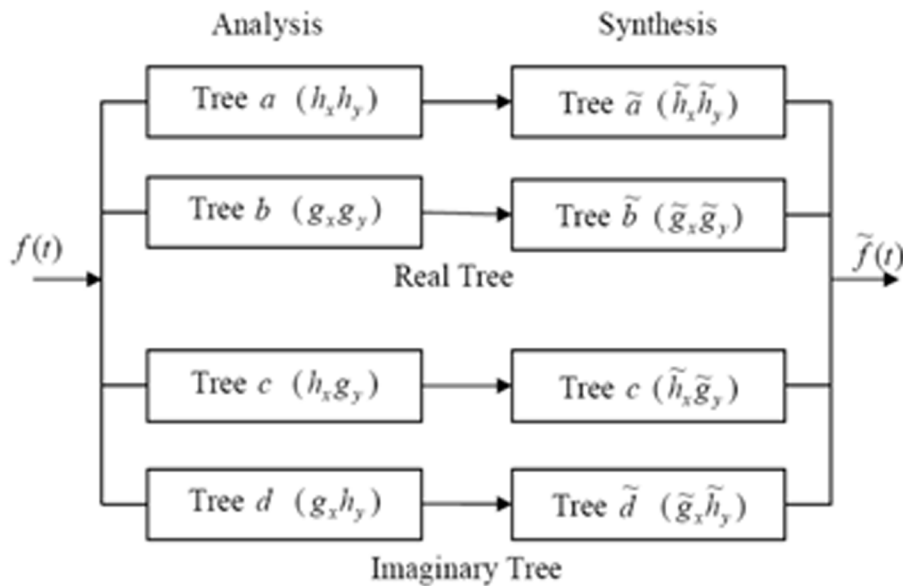


Figure 4: Filter Bank Structure for 2D DT-CWT

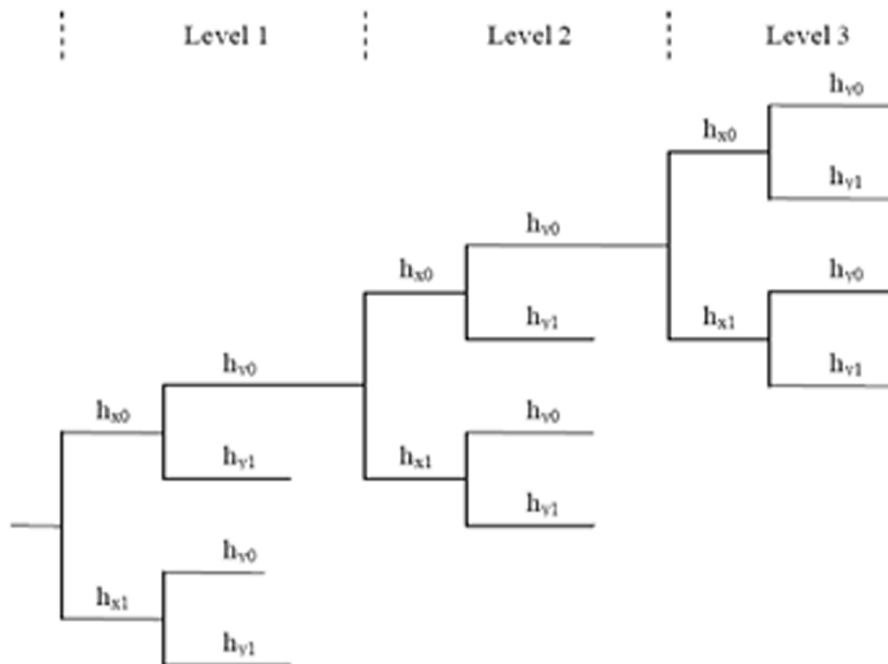


Figure 5: Filter Bank Structure of Tree a

$$(h_x + jg_x)(h_y + jg_y) = (h_x h_y - g_x g_y) + j(h_x g_y + g_x h_y)$$

In fig. 5, the filter bank structure of tree a, similar to standard 2D DWT spanned over 3 level is shown.

For row- and column- filtering, the structure of the other trees -(b, c & d) are combined with the filters. The 2D dual-tree structure is 4-times expensive or redundant compared with the standard 2D DWT. In an analysis filter bank, tree-c and tree-d forms the imaginary pair and tree- and tree-b makes the real pair. With respective to the analysis pair, Trees- $(\tilde{a}, \tilde{b})$  and trees- $(\tilde{c}, \tilde{d})$  forms a corresponding real and imaginary pairs in the synthesis filter bank respectively Selesnick (2001).

To decide whether the non-uniform coefficient is an imaginary or a dual tree, the 2D DT-CWT approach utilizes Fuzzy Inference Filter (FIF) Yang et al. (1995); Farbiz et al. (2000). For modeling fuzzy rules, a general if-then-else structure is used. With basic fuzzy rules and fired coefficients, a dual tree-real coefficient of a sub band is put as co-efficient entropy. Thus, non-uniformity is employed to limit the coefficient sensitivity in a dual tree real root. Fig. 6 illustrates the membership functions and fuzzy rules to compute the wavelet trees entropies and explained as below:

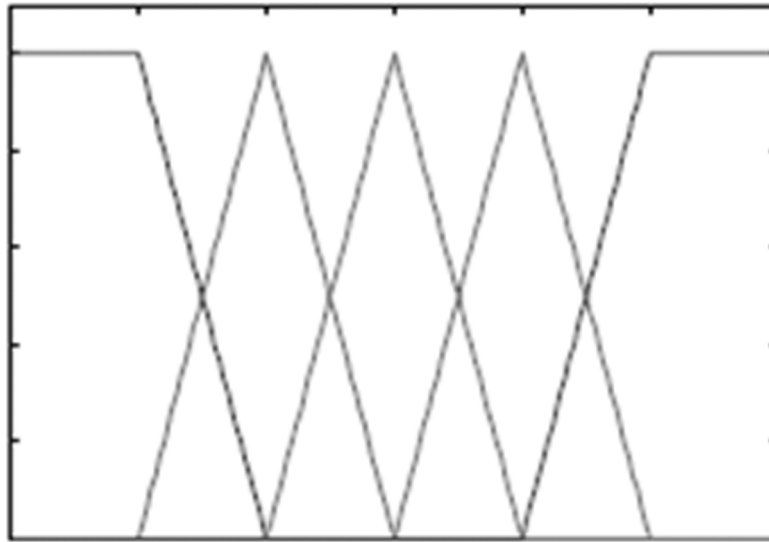


Figure 6: Membership Functions

### 3.4. The Fuzzy Inference Filter

Five fuzzy production rules are engaged as the inference filter as follows.

- $R_1$  : If more of  $X_j$  are Very High, then  $En(x_j)$  is Very High.
- $R_2$  : If more of  $X_j$  are High, then  $En(x_j)$  is High.
- $R_3$  : If more of  $X_j$  are Medium, then  $En(x_j)$  is Medium.
- $R_4$  : If more of  $X_j$  are Low, then  $En(x_j)$  is Low.
- $R_5$  : If more of  $X_j$  are Very Low, then  $En(x_j)$  is Very Low.

In the exceeding production rules,  $X_j \rightarrow$  wavelet tree and  $x_j \rightarrow$  tree root. All coefficients in  $X_j \rightarrow$  the normalized fuzzy coefficients (NFCs) were normalized by dividing by T for user-defined compression quality. Four different levels of compression quality is taken into consideration; and the values of T are defined based on different quality while compression.

$T = t$  for compression quality  $\rightarrow$  low;

$T = t/\sqrt{2}$  for compression quality  $\rightarrow$  medium;

$T = t/\sqrt{2}$  for compression quality  $\rightarrow$  high;

$T = t/(2\sqrt{2})$  for compression quality  $\rightarrow$  very high,

Where  $t = \text{Mean}(\text{Abs}(\text{values of coefficients in HL4}))$ .

The degree of fuzzy membership in the predicate and conclusion parts of the production rules, ‘Very High’, ‘High’, ‘Medium’, ‘Low’, and ‘Very Low’ is illustrated in fig. 6. The entropy of is referred as the filter output  $En(x_j)$ , which represents the degree of membership for  $x_j$  and descendants.

### 3.5. Lattice Vector Quantization

Instead of single pixels, a vector quantizer is utilized for pixel sequences quantization. A vector quantizer with size  $L$  and dimension  $n$  is given as function which maps arbitrary vector  $X \in R^n$  into output vectors  $Y_1, Y_2, \dots, Y_L$  thus known as code vectors belongs to  $R^n$ . The  $L$  code vectors specify the vector quantizer completely and non overlapping partitions of  $R^n$  is given by Voronoi regions.

A lattice  $L$  in  $R^n$  consists of integral combinations of a set of linearly independent vectors. That is given by,

$$L = \{Y \mid Y = u_1 a_1 + \dots + u_n a_n\}$$

Where  $\{a_1, \dots, a_n\} \rightarrow$  set of  $n$  linearly dependent vectors,

$$\{u_1, \dots, u_n\} \rightarrow \text{integers.}$$

A lattice coset  $\Lambda$ , is obtained from a lattice  $L$  by adding fixed translation vector  $t$  to the points of lattice

$$\Lambda = \{Y \mid Y = u_1 a_1 + \dots + u_n a_n + t\}$$

Around each point  $Y_i$  in a lattice coset  $\Lambda$ , its Voronoi region is represented as

$$V(\Lambda, Y_i) = \left\{ X \in \frac{R^n}{\|X - Y_i\|} \leq \|X - Y_j\|, \forall Y_j \neq Y_i \in \Lambda \right\}$$

By choosing finite number of lattice point from an infinite lattice, a codebook of a lattice quantizer is generated. An LVQ codebook is resolute by a root lattice, a scaling factor and truncation. The codebook is actually formulated from the root lattice known as lattice coset. To choose a finite number of lattice points, truncation must be used in a root lattice and by quantizing the input data with finite amount of energy. With the number of points in the truncated area, the bit rate of the LVQ is provided. To provide proper accommodation to the probability distribution of the source, lattice should be truncated and scaled properly. For performing this, it is important to know the availability of lattice point in the truncated area, i.e. to have the acquaintance of the shape of the truncated area.

### 3.6. CABAC Entropy Coding

Entropy coding is a outward appearance of lossless compression employed at the final stage of wavelet coefficients encoding, on the occasion the lessening of the image has been done to a sequence of syntax elements. Syntax elements describe the image coefficients and can be renovated at the decoder. This is comprehensive of the method of prediction and prediction error, also known as residual (e.g., spatial or temporal prediction, motion vectors and intra prediction mode). CABAC comprises of three significant functions: context modeling, binarization and arithmetic coding. Binarization does the charting of syntax elements to binary symbols (bins). Context modeling does the evaluation of the probability of the bins. Finally, arithmetic coding squeezes the bins to bits with the origin of the estimated probability.



### 3.7. Binarization

Binary Arithmetic Coding is employed by CABAC to indicate the encoded binary decisions (1 or 0). Before arithmetic coding, a non-binary-valued symbol is either “binarized” or modified (e.g. a transform coefficient or motion vector). The above mentioned process is similar to the process of transforming a data symbol into a variable length code even if the binary code is encoded before transmission (by the arithmetic coder). For each bit (or “bin”) of binarized symbol stages are repeated. The syntax element provided by the binarization process must be near to the minimum redundancy code in a binary representation. Thus it provides easy access of symbols through binary decisions placed near the root node of the next modeling stage. The code tree reduces the average number of binary symbols for encoding, thus the computational workload is reduced by the provided binary arithmetic coding stage.

### 3.8. Context Modeling

To achieve high coding efficiency, an accurate probability estimated with respect to the Context modeling. The context of the model is updated frequently, with the values based on the earlier coded bins by utilizing the context models and adaptive for different bins. With similar distributions frequently bins share the identical context model. In accordance with the type of syntax element, luma/chroma, neighboring information and bin position in syntax element (binIdx) etc. the context model in each bin is chosen. A context switch can be experiential after each bin.

### 3.9. Arithmetic Coding

Arithmetic coding is given in accordance with the recursive interval division. With basis of probability bin, the intervals are divided into sub intervals with initial value range between 0 and 1. An offset value is yielded by the encoded bits when converting it to binary fraction; it chooses one of the subinterval values, indicating the decoding bin value. The range is equivalently updated after decoding bin to select the sub intervals. Iteration of internal process divides the interval. The offset and the range has reduced bit precision; to avoid underflow, renormalization is performed to eliminate value goes below the range.

## 4. RESULTS AND DISCUSSION

In this division, the proposed 2D DT-CWT based image compression results are evaluated and it is compared with the existing JPEG2000 and 2D-OWT Bo Li et al. (2011). The performance is calculated on the basis of the Mean Square Error (MSE), Compression Ratio (CR), Correlation, Peak Signal to Noise Ratio (PSNR), structural similarity (SSIM), Execution Time.

### 4.1. Dataset Description

Remote sensing image is given as the image extracted from the recording machine which doesn't have the cherished or physical contact with the object under assessment. This remote sensing image is helpful in obtaining the information regarding the area or phenomenon or a target by analyzing the specific information obtained from the remote sensing image. In general it requires the distributing effect or the correction of impertinent sensor features to conduct data analysis. Image acquired from satellite is very useful in various environmental applications like geographical mapping, prediction of agriculture crops, tracking of earth resources, urban growth etc. thereby this paper presents elevation of remote sensing image. It is downloaded from <http://www.spaceimaging.com>.

### 4.2. Performance Measures

#### 4.2.1. Mean Square Error (MSE)

Mean Square Error (MSE) is a simple image quality measurement. The higher value of MSE indicates that the image is in poor quality Walker (2001). MSE is given as follows:

$$MSE = \frac{1}{MN} \sum_{m=1}^M \sum_{n=1}^N (x(m,n) - \hat{x}(m,n))^2$$

#### 4.2.2. Peak Signal to Noise Ratio (PSNR)

If the Peak Signal to Noise Ratio (PSNR) is smaller the image is in poor quality. In general, a high quality reconstructed image is of high PSNR and low MSE. PSNR is given by:

$$PSNR = \frac{10 \log 255^2}{MSE}$$

#### 4.2.3. Correlation

The proximity of two images can be computed with the correlation coefficient. The correlation coefficient is considered using the equation below.

$$\text{corr} \left( \frac{A}{B} \right) = \frac{\sum_{i=1}^M \sum_{j=1}^N (A_{i,j} - \bar{A})(B_{i,j} - \bar{B})}{\sqrt{\sum_{i=1}^M \sum_{j=1}^N (A_{i,j} - \bar{A})^2 \sum_{i=1}^M \sum_{j=1}^N (B_{i,j} - \bar{B})^2}}$$

The correlation is the measure of degree of association between the variables and given by -1 and +1, which represents X and Y. The positive correlation value indicates the large value intended to large value of positive association and the small value of X intended to correspond with the small value of Y. A negative correlation value indicates the inverse or negative association where large value of X is supposed to relate with the small value of Y and vice versa.

#### 4.2.4. Structural Similarity Measures

The similarity between the two images is measured with the structural similarity (SSIM) index. The windows X and Y are a measure of common size  $N \times N$  is:

$$SSIM = \frac{(2\mu_x\mu_y + C_1)(2\sigma_{xy} + C_2)}{(\mu_x^2 + \mu_y^2 + C_1)(\sigma_x^2 + \sigma_y^2 + C_1)}$$

Where  $\mu_x \rightarrow$  average of  $x$ ,  $\mu_y \rightarrow$  average of  $y$ ,  $\sigma_x^2$  is variance of  $x$ ,  $\sigma_y^2 \rightarrow$  variance of  $y$ ,  $\sigma_{xy} \rightarrow$  covariance of  $x$  and  $y$ ,  $C_1 = (K_1L)^2$ ,  $C_2 = (K_2L)^2$  two variables become constant for the division with weak denominator.

#### 4.2.5. Execution Time

The comparison of the existing and the JPEG2000, 2D-OWT and 2D-DT-CWT for calculating the executing time is given here respectively. The proposed 2D-DT-CWT delivers high result for the Remote Sensing Images. Using tic toc method execution time is computed.



Figure 7: Comparison of JPEG2000, 3D-OWT and 2D-DTCWT

Fig. 7 illustrates the proposed work. The input image is a test image. For compressing the image the JPEG2000, 2D-OWT and 2D-DTCWT is utilized to have high frequency components. Fig. 6 illustrates the comparison of JPEG2000, 2D-OWT and 2D-DTCWT which gives higher compression. This proves that the proposed 2D-DTCWT has good efficiency while image compression is under process.

**Table 1**  
**Results of CR, PSNR, MSE, Correlation, SSIM, Execution Time Value for JPEG2000**

IMAGES	JPEG2000					
	CR	PSNR	MSE	Correlation	SSIM	Execution Time
Image1	0.9754	32.0620	40.4464	0.9963	0.7150	34.8945
Image2	0.9704	30.5327	57.5189	0.9949	0.8302	25.4131
Image3	0.9633	30.0303	64.5727	0.9947	0.8757	25.3004
Image4	0.9954	31.3066	48.1310	0.9890	0.8502	40.6478
Image5	0.9441	28.8830	51.1242	0.9909	0.8947	17.5411

**Table 2**  
**Results of CR, PSNR, MSE, Correlation, SSIM, Execution Time Value for 2D-OWT**

IMAGES	2D-OWT					
	CR	PSNR	MSE	Correlation	SSIM	Execution Time
Image1	1.0071	34.5064	23.0380	0.9964	0.9194	0.1884
Image2	1.0082	37.4879	21.5955	0.9963	0.9683	0.1919
Image3	1.0076	33.3991	29.7281	0.9951	0.9413	0.2945
Image4	1.0090	35.4889	18.3735	0.9937	0.9431	0.3141
Image5	1.0092	31.1357	32.0626	0.9831	0.8660	0.3254

**TABLE 3**  
**Results of CR, PSNR, MSE, Correlation, SSIM, Execution Time Value for 2D- DTCWT**

IMAGES	2D-DTCWT					
	CR	PSNR	MSE	Correlation	SSIM	Execution Time
Image1	1.0096	36.8641	20.1254	0.9968	0.9202	0.1871
Image2	1.0120	38.4754	17.5841	0.9964	0.9441	0.1888
Image3	1.0142	35.8541	22.8541	0.9961	0.9642	0.1945
Image4	1.0155	36.4147	16.2584	0.9954	0.9547	0.1914
Image5	1.0165	33.2478	28.2561	0.9848	0.9321	0.1895



**Figure 8: Comparison of PSNR in JPEG2000, 2D-OWT and 2D-DTCWT**

Fig. 8 shows the PSNR comparison between the existing JPEG2000 and 2D-OWT with the proposed 2D-DTCWT. The proposed approach illustrates the higher value of Peak Signal to Noise Ratio (PSNR). From the outcome, it is identified that the proposed 2D-DTCWT method has higher PSNR with high quality reconstructed image.

Fig. 9 demonstrates the comparison of MSE between the available JPEG2000 and 2D-OWT and the presented 2D-DTCWT technique. The proposed method shows lower MSE value. To exhibit good construction image, the 2D-DTCWT retains lower MSE value.

Fig. 10 shows the correlation comparison between the existing JPEG2000 and 2D-OWT with the proposed 2D-DTCWT technique. The proposed 2D-DTCWT projects higher correlation value. From the extracted result, it is shown that the proposed 2D-DTCWT attains better performance when compared to the existing method.

Fig. 11 demonstrates the SSIM comparative results of existing JPEG2000 and 2D-OWT with the proposed 2D-DTCWT. The proposed method shows higher SSIM value. From the result attained the proposed method shows good SSIM compared to the existing method.

Fig. 12 demonstrates the comparison of execution time between the already availing JPEG2000 and 2D-OWT with the proposed 2D-DTCWT technique. The proposed technique shows lower execution time.

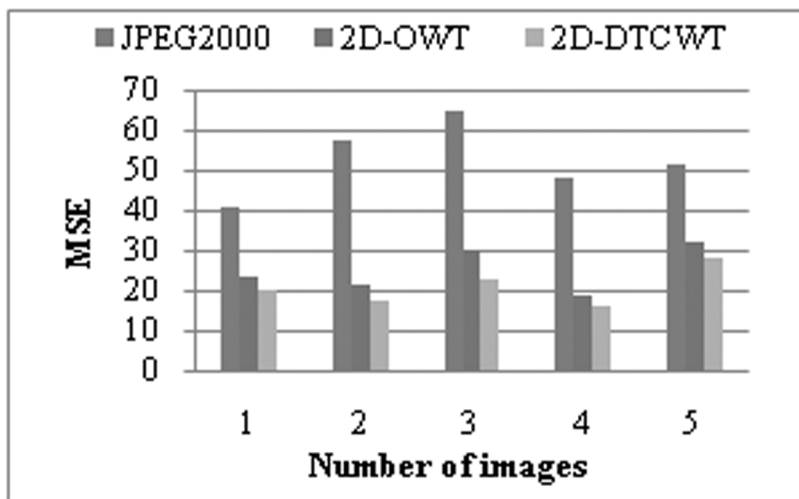


Figure 9: Comparison of MSE in JPEG2000, 2D-OWT and 2D-DTCWT

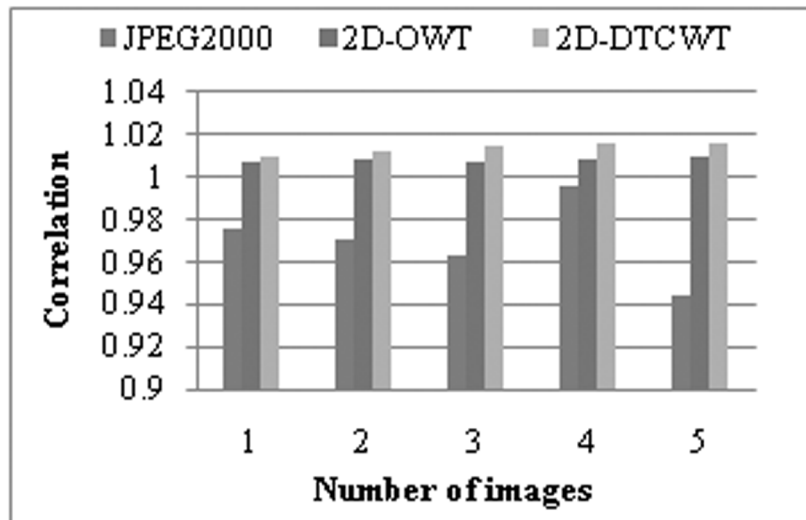


Figure 10: comparison of correlation in JPEG2000, 2D-OWT and 2D-DTCWT

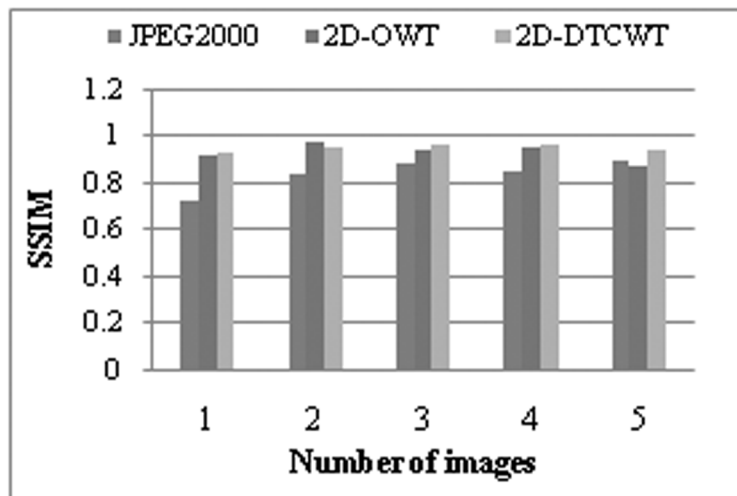


Figure 11: comparison of SSIM in JPEG2000, 2D-OWT and 2D-DTCWT

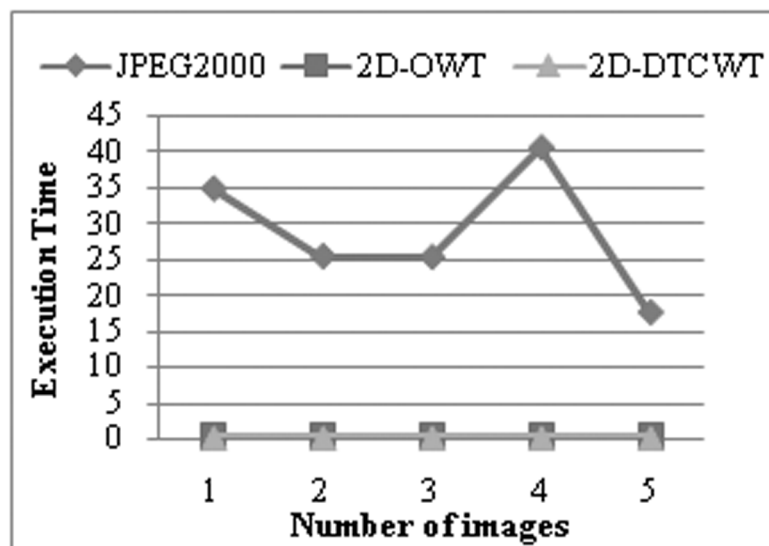


Figure 12: comparison of execution time in JPEG2000, 2D-OWT and 2D-DTCWT

From the attained results, the proposed 2D-DTCWT use only lower execution time compared to the existing method.

## 5. CONCLUSION

Compression increases the significant growth in the field of computing for reducing the size of image or data with minimum storage space and rapid transmission than compressed image or data. Compression in remote sensing image is very essential while faster transmission and minimal storage space. Several methods has been designed for image compression, especially the 2D-Dual Tree-Complex Wavelet Transform (DT-CWT) based image compression algorithm is initiated for compression in remote sensing image. Here in 2D- CWT, wavelet coefficient decomposing of image is initiated first. By applying Fuzzy Interference Filter (FIF), the coefficient values are chosen. It improves the compression ratio. For encoding wavelet significant coefficients, a Context-adaptive binary arithmetic coding (CABAC) with Lattice Vector Quantization (LVQ) is presented. To achieve the superiority quality of the decoded image, a transform based compression algorithm is proposed. When compared with the existing JPEG2000 and 2-D OWT compression techniques, the proposed 2D-DTCWT compression technique is more desirable for remote sensing. The concert of PSNR, CR, correlation values are greater compared to the existing compression

algorithms. Future works will be focused mainly on the new compression techniques based wavelet transform, which may be compared with the 2D-DTCWT compression technique and also concentrate on other criteria's such as compression ratio and PSNR.

## REFERENCES

- [1] Penna, B., Tillo, T., Magli, E., & Olmo, G., (2007). Transform coding techniques for lossy hyperspectral data compression. *IEEE Trans. Geosci. Remote Sens.*, 45(5).1408–1421.
- [2] Taubman, D., & Marcellin, M. (2001). *JPEG 2000: Image Compression Fundamentals, Standards and Practice*. Norwell, MA: Kluwer.
- [3] Taubman, D. (2000). High-performance scalable image compression with EBCOT. *IEEE Trans.*
- [4] Selesnick, I.W., Baraniuk, R.G., & Kingsbury, N.G., (2005). The dual tree complex wavelet transform. *IEEE Signal Processing Magazine*, 22(6).123–151.
- [5] Grgic S.,& Grgic,M., (2001). Performance of Image Compression Using Wavelet. *IEEE Transaction on Industrial Electronics*, 48(3).
- [6] Barbara Penna, Tammam Tillo, Enrico Magli, & Gabriella Olmo. (2007). Transform coding techniques for lossy hyperspectral data compression. *IEEE Transactions On Geoscience And Remote Sensing*, 45(5).
- [7] Jacob, N., & Martin A., (2004). *Image Denoising In the Wavelet Domain Using Wiener Filtering*. Unpublished course project, University of Wisconsin, Madison, Wisconsin, USA.
- [8] Selesnick, I.W., (2001). Hilbert Transform Pairs of Wavelet Bases. *IEEE Signal Processing Letters*, 8(6).170-173.
- [9] Yang, X., &Toh, P.S., (1995). Adaptive fuzzy multilevel median filter. *IEEE Trans. Image Processing*, 4(5). 680-682.
- [10] Farbiz, F., Menhaj, M.B., Motamedi, S.A., &Hagan M.T. (2000). A new fuzzy logic filter for image enhancement. *IEEE Trans. Systems, Man, and Cybernetics*, 30(1).110-119.
- [11] Bo Li, Rui Yang, Hongxu Jiang. (2011). Remote-Sensing Image Compression Using Two-Dimensional Oriented Wavelet Transform. *IEEE transactions on geoscience and remote sensing*, 49(1).
- [12] Walker. (2001). *Wavelet-based Image Compression*. Transforms and Data Compression.
- [13] Khashman, A., and Dimililer, K (2008). *Image Compression using Neural Networks and Haar Wavelet*, WSEAS Transactions on Image Processing, 4(5), 330-339.
- [14] Debnath, J.K.; Rahim, N.M.S. and Wai-keung Fung, (2008). A modified Vector Quantization based image compression technique using wavelet transform, Neural Networks, 2008. IEEE World Congress on Computational Intelligence), 171–176.

